

FINAL PHASE 1 RESEARCH REPORT – METHODOLOGIES FOR GPFA-AB

The Phase 1 Final Report contains a discussion of the methodologies used for each of the major project tasks in GPFA-AB, including process flow charts. This document provides further details and references a series of research memos that were written throughout the course of the project. These memos provide the reader with a still deeper understanding still of the hypotheses, methods, analyses, etc. for various topics.

Methodology Task 1, Thermal Analysis:

Analysis of abundant oil and gas bottom-hole temperatures (BHTs) and sparse equilibrium temperature data (Spicer, 1964; Whealton, 2015) is the foundation for the geothermal resource assessment. As of October, 2014 over 40,000 BHT records were available from the National Geothermal Data System (NGDS) for New York, Pennsylvania, West Virginia, and a 50 km buffer into neighboring Appalachian Basin states. The NY, PA, and WV data were all cross checked with state oil and gas datasets for additional BHT information. Overall, state databases provided redundant temperature-depth information, so the NGDS data was used nearly exclusively for BHT data in this project. This temperature data was merged into a single database with common field headers (see [Thermal Model Memo](#) for details). After eliminating data for quality control reasons, selecting to analyze only wells deeper than 1000 m, and ensuring that each spatial location had only one data point, the data set included approximately 13,300 temperature-at-depth points, prior to spatial outlier detection tests. Spatial outlier tests were performed on each thermal property for which a map was made, and on average removed about 1000 additional points (see [Outlier Memo for details](#)).

BHT data are known to have many potential sources of error, including collection prior to the thermal field returning to equilibrium conditions post-drilling. A set of BHT correction equations were developed that reflect spatial variations in the data and the underlying geology; a detailed description is given in the [BHT Correction Memo](#) in the Catalog of Supporting Files. Broadly speaking, a set of wells were identified with a thermal log that was interpreted as being of better quality (closer to equilibrium) than the surrounding BHT data. There were 48 equilibrium logs available; these were grouped into 24 clusters, and neighboring BHTs were corrected to the estimated equilibrium temperature profile. Further analysis showed that the BHT corrections followed systematic patterns depending on geological province, and on that basis a small set of temperature correction functions were established and applied to all the remaining wells.

Estimations of heat flow and the temperature field at depth requires knowledge of the “conductivity stratigraphy” at the >13,300 boreholes whose BHT data were used. We assigned lithologic units, thicknesses of each unit, and corresponding thermal conductivities to each borehole from the surface to the basement. To accomplish this in the time available, we used the AAPG (1985a, 1985b) COSUNA lithology charts and regional maps published by the Trenton Black-River Project of the depth to basement, above which the COSUNA information was applicable. Full details are given in the [COSUNA Methodology Memo](#) in the Catalog of Supporting Files. (West Virginia Geological & Economic Survey, 2006). In the absence of detailed information regarding the thermal conductivity values of the Appalachian basin sedimentary rocks, values of conductivity for similar rock compositions from the geologically similar Anadarko Basin were used. Refer to both the [COSUNA Methodology](#) and [Anadarko Basin Thermal Conductivity Memos](#) for further details.

To transform the depth-specific and well-specific corrected BHT data into uniform thermal metrics, a computer program was developed to calculate the surface heat flow, and the geotherm (i.e. temperatures at depth) for all wells with BHTs and stratigraphic information. This program is a steady state, 1-D heat conduction model (Jaeger, 1965) that was developed and tested in the open source software program Python 2.7.9 (see the [Thermal Model Methods Memo](#) for details). This model updates and improves upon previous work by Cornell and SMU as part of the Google.org and NGDS projects (Blackwell D. D. et al., 2011); (Stutz G. R. et al., 2012). This model assumes that radiogenic heat production is constant and uniformly distributed in sedimentary rocks, and dies off exponentially in the basement crustal rocks as per Lachenbruch (1968). A constant mantle heat flow of 30 mW/m² is assumed to be present throughout the region based on the average mantle heat flow for the stable continents, including the Appalachian Basin (Roy, Blackwell, & Decker, 1972).

The inputs to the thermal model involve a variety of simplifications and assumptions. To evaluate the robustness of the output, Monte Carlo simulations were used to examine the variability of the predicted thermal properties as functions of the uncertainties of the input variables. One topic of broad uncertainty was the reliability of using the simplified conductivity stratigraphy based on the regional COSUNA lithologic simplification. To examine the consequences of this simplified method, we obtained well-specific conductivity stratigraphy data for 77 wells, distributed widely across the study area ([Tests of Simplified Conductivity Stratigraphy Memo](#)). These well data and the COSUNA-based simplified data for the same wells were each subjected to Monte Carlo simulations, and the thermal predictions compared.

Using the results from the 1-D model, a local outlier analysis was run on each calculated thermal variable ([Thermal Outlier Assessment Memo](#)), and were then subject to a spatial interpolation to generate the predicted mean and the standard error of the predicted mean for the resource, and create maps representing the thermal quality in a GeoTIFF format. Within the Appalachian Basin, wells are clustered where there are oil and gas reservoirs, and sparse in areas with little to no oil and gas exploration. Therefore, interpolation algorithms must be able to handle predictions for sparse and clustered data. The spatial interpolation used in this analysis is so-called stratified¹ ordinary Kriging implemented in the open source language R in the package gstat (Pebesma & Wesseling, 1998; [Interpolation Methodology Memo](#)). Lateral regional boundaries were defined based on natural geological boundaries, defined by gravity field and magnetic field data at depths from 18 km to 34 km ([Interpolation Methodology Memo](#)). These geologic boundaries should enclose rocks with similar properties, and may represent small-scale “heat flow provinces” (Roy, Blackwell, & Birch, 1968) Statistically, lateral stratification/regionalization preserves this assumption by interpolating data separately for all provinces, which potentially have different data generating processes (e.g. differences in thermal conductivity, heat generation, mantle heat flow, etc.).

The Kriging algorithm considers the spatial autocorrelation in the variable to be predicted, with the expectation that points closer to one another are more similar in value than points farther away. Variograms corresponding to this structure of spatial (semi)variance illuminate differences on spatial scales smaller than the entire Appalachian basin. This result justifies the decision to model BHT corrections and the thermal map interpolations on local scales rather than on a global scale. The stratified/ interpolations capture this variability to provide the predicted mean and the spatial standard error of the predicted mean for each thermal variable calculated using the thermal model. For interpolations, the spatial correlation range (distance) was used as the maximum searching distance for nearest neighbor points – beyond this range there is no modeled spatial correlation. In addition to the searching distance restriction, a minimum of 5

¹ “Stratified” in this geostatistical context means an analysis regionalized by lateral boundaries. To other geoscientists, that terminology is a source of confusion since strata means vertical layering rather than lateral boundaries.

points were required to make a prediction at any location within the basin. As a result of these interpolation restrictions and the 1000 m cutoff depth, some areas on the thermal map do not have predictions. For example, Allegheny National Forest in Pennsylvania has limited deep well data, and therefore appears white on the thermal maps.

Maps were prepared that express the regional variations in surface heat flow, the depths to an 80 °C surface and to a 100 °C surface, and the temperatures at depths of 1500 m, 2500 m, and 3500 m. A leave-one-out cross validation was performed for each of the interpolated thermal variables, with the result that about 98% of the values of left-out points were contained within 3 standard errors of the predicted mean for that thermal resource (see the [Tests of Simplified Conductivity Stratigraphy Memo](#) for the results of the cross validation in each of the 12 selected counties). Another evaluation of the interpolation performance was through comparison of equilibrium temperature logs at 1.5 km to the predicted mean at 1.5 km (Figure 18 in main body of the report).

The mapped heat resources were ranked by 3-level (Green/Yellow/Red) and 5-level (Green/Greenish-yellow/Yellow/Orange/Red) divisions. The thresholds could be selected based on either general economic considerations, in that costs for geothermal energy projects rise as the depth needed to reach the temperature of interest increases, or based on the temperature requirements of a given end-use technology ([Thermal Resource Thresholds Memo](#)). For a 5-division scheme for maps showing the depth to a selected temperature, the threshold to least favorable (red) conditions is set at a production depth that would cost approximately \$10 million to drill and complete a well, which for current estimates of drilling costs corresponds to an average depth of about 4000 m. The succession of thresholds for improved quality of the thermal resource were selected in approximately \$2 million cost increments. For a 5-division scheme for maps showing the temperature at selected depths, thresholds were selected based on the end-use temperatures, or favorable values of the geothermal gradient at the depth of interest (e.g. 1.5 km). Thresholds are different for each depth considered because the favorability in temperature changes with depth. The threshold to least favorable (red) conditions are set at or below 50 °C, the minimum useful temperature. The most favorable (green) conditions are set between 90 °C (for 1.5 km depth) and 150 °C (for 3.5 km depth). Thresholds in between these depths are selected based on end use temperatures for certain projects.

Measurements of Thermal Conductivity

Specific to thermal conductivity, the Appalachian Basin did not have sufficient data available during Phase 1 to select representative values for each lithology encountered in the basin. The Anadarko Basin thermal conductivity samples were chosen as representative to the Appalachian Basin because of the similarities between the paleo-burial depth and age of the two basins. Thermal conductivity is strongly influenced by depth of burial (decrease in porosity), and these basins reached similar burial depths. During the past year, original samples from Carter et al. (1998) were rerun at SMU to confirm our understanding of certain formation values differing by more than 10% in the Carter et al. (1998) paper (see [Anadarko Basin Thermal Conductivities Memo](#)). The thermal conductivity of a formation, when measured on a divided bar, have had reported differences between samples of ± 5 to 10% depending on the formation (Gallardo & Blackwell, 1999; Carter et al., 1998). This reexamination of Carter et al (1998) data highlighted how the mineralogy of the rock sample can change even at the meter scale, thereby impacting the thermal conductivity on scales smaller than are of interest for this stage of the project. For this project, formation thermal conductivity on average is of interest, so the values from Carter et al. (1998) and available Appalachian Basin thermal conductivities were subject to a Monte Carlo simulation to obtain formation specific average thermal conductivities and measures of uncertainty variance. These values were used to construct the COSUNA

based thermal conductivity stratigraphy for use in the 1-D heat conduction model. In the thermal model, over the entire well the thermal conductivity is weighted by formation thickness and harmonically averaged as part of the heat flow and geotherm calculation. In an effort to move away from Anadarko Basin thermal conductivities, during Phase 2 we want to run additional core samples for the formations of interest in the Appalachian Basin to confirm that our assigned values are appropriate, or to change them. The thermal conductivities of Appalachian basin samples can be analyzed at SMU or WVU.

Methodology Task 2, Natural Reservoir Quality:

Task 2 for this project involves the mapping and characterization of natural reservoirs within the Appalachian Basin region of New York (NY), Pennsylvania (PA), and West Virginia (WV). Phase 1 of this project was limited to the analysis of existing data. Because drilling for oil and gas in the Appalachian Basin has taken place for over a century, the petroleum industry has vast amounts of data for reservoirs. For the purpose of Phase 1, only proven hydrocarbon reservoirs were considered; future work may include the consideration of dry, or non-producing, reservoirs.

The oil and gas industry uses the term field to describe a group of wells that all penetrate into the same formation to produce oil or gas; therefore, all sources of data for this project used the term field. However, in the geothermal industry, the term reservoir is more commonly used, to mean a given volume of heated and permeable rock from which heat can be extracted using circulation of fluids. A field and a reservoir are essentially the same thing, but the perspective is shifted from the wells to the entire body of rock. All cases where the term field was encountered in our original datasets were changed to reservoir for the remainder of the project.

After thermal quality, injection flow rate is the second-most important factor affecting geothermal heat production (Bedre & Anderson, 2012). However, because flow rate is highly dependent on engineering and operational selections, it is a difficult reservoir metric to estimate with reservoir parameters alone. The challenge, therefore, was to develop a reservoir metric that considers flow rate but is described using only reservoir parameters, including porosity and permeability, depth, and reservoir thickness and area.

The oil and gas industry, from which we collected the majority of our data, does not need to produce or inject fluids at an ongoing basis of geothermal magnitude (e.g., >300,000 gpd or 30 kg/s), therefore the industry does not report maximum fluid flow rates from their wells. The end product assigned to the reservoirs is the Reservoir Productivity Index (RPI), which is related to the expected productivity index of a given well, taking into account the permeability, thickness, water viscosity, and area, as a means to estimate the ratio of flow rate to pressure drop.

This project analysis of natural reservoirs included more parameters than previously reported in the existing National Geothermal Data System (NGDS) content model for Geologic Reservoir Analysis, developed by the Texas Bureau of Economic Geology. One new parameter is “Reservoir Productivity Index” (RPI), a new metric adapted from the productivity index of a well, in units of L/MPa-s. Reservoir permeability, depth, area, and thickness are used to calculate a reservoir's most likely Reservoir Productivity Index using a Monte Carlo Simulation. Instead of simply adding a field called RPI to the existing content model for Geologic Reservoirs, we updated the entire content model and added flexibility for numerous types of analysis projects to provide relevant reservoir data. Researchers can now use the content model to report “*Reservoir Favorability*”² and describe the units and methods associated in their analysis – in our case RPI in L/MPa-s. This is just one example of many such updates; the revised NGDS Geologic Reservoir Content Model is now available on USGIN (U.S. Geoscience Information Network, 2015) for others to use.

Key Assumptions, Reservoir Favorability:

- Porous media flow approximation for all reservoirs
- Geologic formation thickness is a proxy for geothermal reservoir thickness
- Reservoirs in New York (which did not have porosity data associated with them) were assigned the same porosity value across similar geologic formations

Primary Steps, Reservoir Favorability:

1. Compile all existing datasets from the oil and gas industry
2. Amalgamate the data across the three states, including reconciling differences in data collection styles/methods and inputting missing values where needed
3. Research porosity and permeability values for all reservoirs in NY; research porosity-permeability relationships, or average permeability values where relationships were unavailable, for reservoirs in PA/WV.
4. Create polygons in GIS for NY reservoirs using well locations.
5. Research geothermal reservoir metrics and develop a useful favorability index for this project's reservoirs (Reservoir Productivity Index--RPI)
6. Develop an uncertainty index for reservoir data source and quality, and assign values to all reservoir's parameters.
7. Determine best metric to illustrate reservoir uncertainty in map-view. Choice was Coefficient of Variation (standard deviation divided by mean)
8. Conduct a Monte Carlo Simulation to calculate most likely Reservoir Productivity Index for each reservoir.
9. Display results for RPI and uncertainty in a GIS.

Strengths of Reservoir Favorability Determination Process:

- Compares any and all reservoirs in a basin to each other using reservoir properties only.
- Compares reservoirs based on properties that are important to flow rate, which is the most important quality of a reservoir

² The Content Model defines **ReservoirFavorability** as “Calculated expression of the reservoir's favorability for geothermal applications. Examples of suitable parameters include flow rate, productivity, etc. Chosen parameter description and units need to be provided in methodology field. Uncertainty and methodology are required if **ReservoirFavorability** is provided.” **ReservoirFavorabilityUncertainty** is defined as “An expression of the confidence in the **ReservoirFavorability** value. Best practice to include units and assumptions for calculating uncertainty within **ReservoirFavorabilityMethodology**.” **ReservoirFavorabilityMethodology** is defined as “The method for calculating **ReservoirFavorability** is stated here. Required if **ReservoirFavorability** is provided, to explain units and calculation of **ReservoirFavorability**. Also provide units and method for calculating **ReservoirFavorabilityUncertainty**.”

- Removes temperature from the solution; the reservoir and temperature maps are mutually exclusive, intended to be combined only at the end of the project when all risk factors are combined.
- Uncertainty Index is a great tool to account for differences in quality and source of data from state to state, formation to formation, and reservoir to reservoir.
- Coefficient of Variation is a great tool to compare the uncertainty of each reservoir to all other reservoirs, in a normalized manner.
- Monte Carlo Simulation provides the ‘most likely’ value of RPI, given the assigned Uncertainty Index of each reservoir parameter, thereby eliminating the ‘one-solution’ obstacle to a complex problem
- Does not remove any reservoirs from the population until after the Monte Carlo Simulation is complete. (this is excluding very shallow reservoirs in PA/WV, which were removed for ease of database compilation)

Limitations of Reservoir Favorability Determination Process:

- Many reservoirs overlap in map view, so maps were made at different intervals to better display results.
- The RPI equation applies to porous media formations only. A comparable equation for fractured reservoirs could not be derived.
- It is difficult to see small reservoirs (such as those in PA) on a zoomed out map scale. This problem of small reservoirs is attributed to differences in methods for creating oil and gas field polygons from one state to another.

Mathematical components of Reservoir Favorability Determination:

The petroleum industry often uses a term called the well productivity index (PI) to quantify the productivity of a given oil or gas well producing from a reservoir that is dominated by matrix, or intergranular, flow. The PI is defined as the volumetric flow rate of a well divided by the pressure drop from the reservoir to the producing well, shown as follows:

$$PI = \frac{Q}{\Delta P} \left(\frac{m^3}{Pa-s} \right) = \frac{2\pi kH}{\mu \ln \frac{D}{r_w}} \quad \text{Equation 1}$$

where Q is flow rate (m³/s), ΔP is the pressure drop from the reservoir to the production well (Pa), k is permeability (m²), h is reservoir thickness (m), μ is the fluid viscosity (Pa-s), D is the distance between the injection and production well (m), and r_w is the wellbore radius (m) (Gringarten, 1978).

PI has also been used to characterize the productivity of well doublet geothermal reservoirs, for both EGS reservoirs and sedimentary aquifer reservoirs (Gerard et al., 2006; Sanyal & Butler, 2009; Augustine, 2014; Cho et al., 2015). The reservoir team used a similar metric to the PI to quantify the favorability of our potential sedimentary geothermal reservoirs.

Equation 1 was modified for the purposes of this project in three ways:

- Parameters not pertaining to the reservoir characteristics were omitted: D, r_w.
- Fluid viscosity was retained in the equation, because the depth of the reservoir affects the viscosity of the fluid (temperature effects). For more information, see document “Reservoir Database Inputs”.
- A unitless area factor (fa) was added to the equation to incorporate the effect of reservoir size. For more information, see document “Reservoir Database Inputs”. Reservoirs larger than a specified

threshold were given a larger area factor to boost their favorability. Larger reservoirs may contain more heat, but there may be practical barriers to accessing all the heat from very large reservoirs. For these reasons, the area factor was added to Equation 1.

The final Reservoir Productivity Index (RPI) equation used for this task is as follows. The conversion factor of 10^9 results in a final value in units of liters per MegaPascal-seconds.

$$RPI = \frac{Q}{\Delta P} \left(\frac{L}{MPa-s} \right) = 10^9 * \frac{2\pi kHf_a}{\mu} \quad \text{Equation 2}$$

Potential Sources of Error in Reservoir Favorability Determination:

- Incorrect RPI equation for fracture dominated reservoirs
- Average permeability values taken from literature not accurate
- Porosity-permeability relationships inaccurate

Software Used in Reservoir Favorability Determination:

- QGIS 2.6
- MatLab R2015a

Results of Sensitivity Analyses for Reservoir Favorability Determination:

Permeability is the primary variable affecting RPI; Thickness is the second most important variable. (see Figure 1: Sensitivity Analysis for Reservoir Productivity Index (RPI))

Primary Conclusions of Reservoir Favorability Determination:

As discussed more fully in the section on Primary Conclusions of this report, most reservoirs in the Appalachian Basin have a low calculated RPI (see Figure 2 below), likely due to low permeability in the geologic formations (see sensitivity analysis tornado plot above). Stimulation would likely be required to use low-permeability geologic formations.

There are several geologic formations that have good potential as geothermal reservoirs. These include the Oriskany and Newburg Sandstones in WV; the Onondaga Reef, Devonian Unconformity Play, and Galway Sandstone in PA; and the Trenton-Black River Dolomite and Onondaga Reef in NY. See Figure 1 below, noting that PA reservoirs are very small and difficult to see unless in a GIS:

There are probably many potential reservoirs not displayed on the above map because they did not produce oil or gas, but instead are water-filled or dry porous formations. There is a need to map out and characterize dry reservoirs in a next phase, or perhaps to geologically extrapolate the possible existence of undrilled reservoirs.

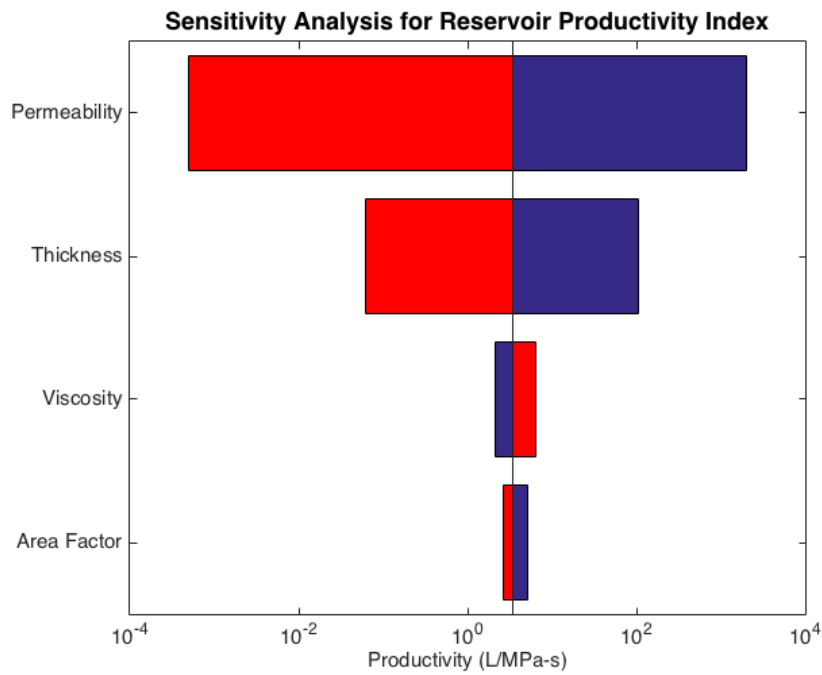


Figure 1: Sensitivity Analysis for Reservoir Productivity Index (RPI)

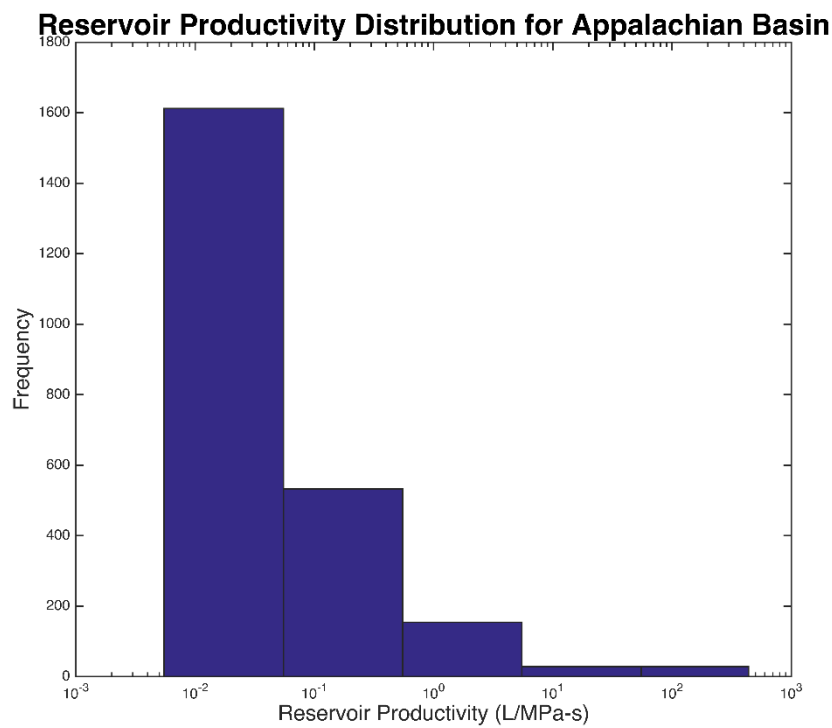


Figure 2: The distribution of reservoirs in the Appalachian Basin ranked by the determined Reservoir Ideality (logarithmic values of L/MPa-s).

Methodology Task 3, Seismic Analysis:

We considered recorded natural seismicity to be a primary indicator of the potential for inducing seismicity in any geothermal developments. To establish the locations and magnitudes of historical events, we combined all relevant data from two high quality seismic catalogs.

The first catalog, from the USGS National Earthquake Information Center (NEIC) provided hypocenter locations from 1965 to the present. A well-known weakness of this source of earthquake data stems from the relative scarcity of recording seismometers for this region of the country. This weakness appears as a relatively high “completeness magnitude” for this data source due to large distances (on average) from events to recorders – implying only larger earthquakes could be identified on enough stations to estimate locations and magnitude. Nevertheless, this catalog – due to its long time span – turned out to provide the majority of earthquakes actually used in our analysis. A major benefit of earthquake events included in this catalog stems from them having been analyzed by expert seismologists to classify the sources as actual earthquakes – as opposed to seismic energy generated from mine or quarry blasting. If an event from our region was categorized as an earthquake in the NEIC, we used it.

The second catalog, the Array Network Facility (ANF) Seismic Bulletin from the National Science Foundation’s EarthScope Transportable Array (TA) rolling deployment provided event locations in our region from approximately the beginning of 2011 through the end of May 2015. The array of broadband seismometers was deployed to temporary sites – with approximately 70 km spacing – and retrieved on a rolling schedule during this time period, so the regional event coverage varied with time. While we did find some events usable for our project from this source (red events in Figure 5 of the [Identifying Potentially Activatable Faults Memo](#)), the lower magnitude catalog completeness we had anticipated in the early stages of the project did not, in fact, play a large role. An unanticipated drawback of this source of earthquake data came from the fact that the ANF bulletin reports all events recorded by the TA, regardless of their source. As described in Astiz et al. (2014), this leads to the inclusion of blasting sources of energy in addition to the naturally occurring earthquakes we are interested in. Indeed, this contamination led us to initially incorrectly identify seismic energy from the West Virginia coal mining regions and elsewhere as naturally occurring earthquakes. With the advice of Beatrice Magnani (SMU), we ameliorated this contamination problem by the rather crude means of simply eliminating TA events from 07:00 to 18:00 (local times) from our analysis – due to Federal mining regulations requiring blasting during daylight hours only. Clearly, this crude decontamination strategy might have eliminated some actual earthquakes. However, just due to raw probabilities from the daily timespans, the odds of keeping a true earthquake event from the TA are 13 in 24 – hence we might have lost a little under half of the true TA recorded earthquakes.

The resulting combined catalog retains all recorded earthquakes with epicenters in our region of interest -- regardless of depth, magnitude, or any other seismic attribute. For consistent quality control, no attempt was made to include either historical (pre-instrumental) seismicity or events from other catalogs such as the ISC. Events from the NEIC (green) and those not rejected by the decontamination procedure from the TA (red) are shown in Figure 7 of the [Identifying Potentially Activatable Faults Memo](#).

As described in great detail in (the [Identifying Potentially Activatable Faults Memo](#)), we used Poisson wavelet multiscale edge (“worm”) analysis of gravity and magnetic grids for a consistent mapping and identification of regional structures on which we anticipate seismicity could potentially occur. Briefly, worms are closely related to the traditional horizontal gradient analyses of potential fields, but a physical interpretation arising from the wavelet technique (e.g. Boschetti et al., 2001; Hornby et al., 2002) allows their classification at depth as candidate faults (see the [Identifying Potentially Activatable Faults Memo](#) for

more detail on the relevant mathematics). The Python based software to calculate worms is open sourced (Horowitz and Gaede, 2014).

We employed two different methods to estimate seismic risk for our region:

1. The first method used both the gravity and magnetic worms as well as the located earthquakes. Here, we simply plotted locations of earthquakes and the worms within a range of horizontal distances. The key idea here being that these locations of structures could unequivocally be classified as potentially active faults. This first method made no attempt at using orientations of the worms – only proximity. The result of this technique is plotted in Figure 7 in the [Identifying Potentially Activatable Faults Memo](#) where all worm points within 5 km of an earthquake location are classified as highest risk; from 5 to 10 km classified as moderately high risk; from 10 to 15 km classified as moderate risk; and from 15 to 20 km classified as moderately low risk. Those distance ranges were selected rather arbitrarily, but we judged them to provide a reasonable tradeoff between prudence and an overabundance of caution – not wanting to sterilize too large a region due to recorded earthquake activity. In the spirit of a play fairway analysis, we anticipate these risk categories to be used simply as a guide to more detailed analysis for any prospective regions. A clear drawback of this technique is that it can only identify active faults based on seismicity from approximately 50 years of instrumental records. This 50 year timespan is of insufficient length to be a representative sampling for earthquake cycles on the order of hundreds of years. However, the fact that these locations are unequivocally sites of active seismicity should play a significant role in determining prospectivity given that seismicity would detrimentally affect any candidate geothermal project's social license to operate.
2. The second method – attempting to fill in some of the spatial and information gaps from the first method – performed in essence a “slip tendency” analysis for the orientations of worms in the regional stress field orientations. Regional stress field orientations were interpolated to each gravity and magnetic worm point using the technique described in Heidbach et al. (2010) – which modifies the directional statistics approach of Mardia (1972) to provide a weighted interpolation. Both the estimated orientation and an estimate of errors are available at every worm point via this method. Worm strike and error estimates were also calculated at every gravity and magnetic worm point according to Mardia's (1972) techniques. From these two orientations and errors, we could then use the Byerlee's (1978) law coefficient of friction (0.85) to derive the worm orientation in the regional stress field most favorably oriented for slip. Angular ranges in increments of 5 degrees around these favorable orientations were then used to classify worm points for seismic risk. Once again, this can only be a qualitative index of risk due to the fact that the actual magnitudes of the state of stress are unknown at our worm points – we only know the orientation with respect to σ_1 . See the [Identifying Potentially Activatable Faults Memo](#) for more details. We appreciate that this index is a “slip tendency” used in other GPFA projects to identify prospective areas, due to fault activity reworking fault gouge to create fresh porosity (and presumably permeability). However in our case, the very same mechanics represent a double-edged sword. Proximal to population centers, seismic risk due to this slip tendency might detrimentally affect a project's social license to operate. Away from population centers, high slip tendency might indeed be a good attribute! Because we are operating under an assumption of direct use geothermal projects, we anticipate any prospectivity in our region would be proximal to populations – and on balance present more of a detriment to a candidate project than a benefit. (Software to perform this analysis against World

Stress Map and worm data stored in the GIS database PostGIS will be available via a Git repository under <https://bitbucket.org/geothermalcode/> shortly.)

An additional attribute – possibly relevant to increasing the footprint of the reservoir analysis – can also be calculated from the same information used for slip tendency. If we define “dilation tendency” to be locations where worms are nearly normal to σ_3 (i.e. parallel to the σ_1 direction), we have an index for the potential locations of mode-I fracture openings. As used in several other GPFA projects, these may well be good locations to explore for fractured reservoirs. We leave further fleshing out and validation of this idea to Phase 2.

The two different methods described in the paragraphs above have quite different qualitative character – and we have an ongoing internal discussion as to which of the two approaches offers more practical utility. Mathematically, the first “earthquake proximity” method represents a sufficient condition for seismic risk, while the second “slip tendency” method represents a necessary condition – at least under the assumptions inherent in applying a Byerlee’s law *model* to the real world. Neither method is simultaneously necessary and sufficient – which would be a logical prerequisite for a completely reliable seismic risk prediction. In the face of this dilemma, we combined the risk estimates from the two by averaging the risks– resulting in Figure 23 in the main report. In our judgment, this combined risk map is likely to be more reliable than either standalone method. This is because it emphasizes those worms proximal to earthquakes that also have high slip tendency. Those are sites it would be prudent to avoid perturbing the ambient effective stresses by injecting fluids. The additional improvement in the spatial footprint of seismic risk due to the slip tendency method in the combined map is also of benefit since it flags areas of concern where geothermal prospects would be wise to perform a detailed state-of-stress analysis from local data.

Methodology Task 4, Utilization Analysis:

The Utilization effort for the Geothermal Play Fairway Analysis of the Appalachian Basin (GPFA-AB) included two broad types of data: 1) residential – community ‘Places’ and 2) site specific users with high heating demands such as universities, industrial users, government facilities, etc. to be considered as part of Phase 2. Below is a description of the data collected, the programs used, and the generalized results of the data processing for the residential – community Places. For the step-by-step descriptions of each parameter and the actual programs, see the Catalog of Supporting Files of this report for the [Utilization Analysis Memo](#).

Steps in Determining the Surface Levelized Cost of Heat

The foundation source code used for the utilization risk assessment is the program GEOPHIRES, (GEOthermal Energy for Production of Electricity and Heat Economically Simulated) (Beckers K. F. et al., 2013; Beckers et al, 2014; Beckers K. F., 2015)). The software uses key data as input to calculate Levelized Cost of Heat (LCOH). Because we have characterized the subsurface as part of other tasks (thermal resources and natural reservoir quality), we modified GEOPHIRES to focus on those remaining elements, which would include demand for heat as calculated from population and climate data, and the surface costs associated with delivering that heat to those in demand. Thus, in our implementation, the final output is a Surface Levelized Cost of Heat (SLCOH). The SLCOH includes the surface piping, heat exchange equipment (residential and/or commercial), operations, upfront capital cost, and maintenance costs over the lifetime of a 30 year project. A MATLAB³ program serves as an interface between the Microsoft Excel

³ <http://www.mathworks.com/products/matlab/>

files of collected input data and the GEOPHIRES program. The GEOPHIRES program can also be used to include the below ground parameters, such as fluid temperature, flow rate, and drilling costs, but these were not included in this cost estimate because they were incorporated in the Natural Reservoir and Thermal Resources sections of the project.

1. The U.S. Census Bureau maintains a database of information that includes state, county, county subdivision, under the broader term 'Place.' A Place is used to identify all individual cities, towns, villages, boroughs, universities, and other Census-Designated Places (CDP's) defined as "settled concentrations of population that are identifiable by name but are not legally incorporated" (Census Bureau, 2012). The population and scope of a single Place may vary from the whole of New York City proper, with a population of over 8,000,000, to the smallest villages with populations as low as 10. In the New York, Pennsylvania, and West Virginia area we are using the 2010 Census data collection that includes 3,355 Places. These were downloaded via the FactFinder website (<http://factfinder.census.gov>).
2. Starting from the New York, Pennsylvania, and West Virginia 3,355 places, using ESRI ArcGIS, the broader Place data were linked to their county and county subdivision. In order to complete this task, shapefiles of the Census Places and county subdivisions were put into ArcGIS. By using a spatial join and having the program find the Places within the county subdivision, this resulted in joining the attributes tables of the two files, allowing for the information for Places to have corresponding county subdivision data. Finally, all sites were checked and any places without a successful join had data manually added. This process was repeated to relate places with county information.
3. The place list was next limited to only those within the project Appalachian Basin outline, which includes 10 km outer buffer. We used the Golden Software program Mapviewer and ArcGIS for a comparison to confirm accuracy of locations within the project boundary. This reduced the number of possible Places for the project to 1,697.
4. For this Play Fairway Analysis project, a minimum population threshold of 4,000 residents per Place was applied for all three states, to focus on those Places with a sufficient number of users to justify the initial capital investment associated with a district heating system. There were 1,449 Places with populations of less than 4,000, leaving the final number of Places for the SLCOH analysis to be 248. In order to have those Places with fewer than 4,000 people appear as red (unfavorable) on the final maps, they were assigned the same arbitrarily high SLCOH of \$100/MMBTU. The actual input data associated with these places would lead to a different SLCOH and can still be calculated for future analyses as appropriate. The population threshold can be set as low as 1,500 residents per Place, and in doing so, makes the majority of the Places meet the criteria of good enough to consider. Although a positive outcome, we determined the 4,000 resident level for population of increased value in focusing the attention to sites most likely to be first users of this new energy concept.

5. The next parameter is the building density and heating demand per building (i.e. detached single-family, attached single-family, 2 unit buildings, 3-4 unit buildings, 5-9 unit buildings, 10-19 unit buildings, 20-49 unit buildings, and 50+ unit buildings). These detailed data are included within the Census Factfinder under “American Community Survey” using the 2010 5-year estimates and code B25024, representing the number and type of housing units per residential building category. The Energy Information Agency (EIA) performs a Residential Energy Consumption Survey (2009) that we used to determine average square footage of each designated unit and related heating load on a Census region basis.
6. Within many Places are commercial buildings, which can be put into 12 categories: 1) Accommodation, 2) Food, & Other Services, 3) Administrative and Waste Management and Remediation Services, 4) Arts, Entertainment, and Recreation, 5) Educational Services, 6) Health Care & Social Assistance, 7) Information Geographic Area Series, 7) Manufacturing, 8) Other Services, 9) Professional Scientific & Technical Services, 10) Real Estate & Rental and Leasing, 11) Retail Trade, and 12) Wholesale Trade.
 - a. In order to determine the heating loads for commercial sites within our Place dataset, we combined the energy consumption for building types, the square footage of a building, and the type of commercial application based on the 12 categories above. Three datasets were used: the EIA’s 2006 report of Commercial Buildings Energy Consumption Survey (CBECS) for the *floor space*, the US Factfinder 2007 ‘Economic Data’ for categories, and the EIA manufacturing *energy consumption* database available at <http://www.eia.gov/consumption/manufacturing/>.
 - b. From these files, the number of establishments and number of employees were collected for each “economic place”. Unfortunately, the term “economic place” did not equate to that of the census definition of Place. The “economic place” can be related to the census classification of “county subdivision”, which we did have linked to each Place. Following the methodology of Reber (2013) and Tester et al. (2015), in the instance where a single “county subdivision” (i.e. “economic place”) contained multiple Places (typically around metropolitan areas) the data on commercial establishments for that county subdivision was divided amongst the Places within that county subdivision based on the relative population of each Place. In addition, due to the potentially identifiable nature of the reported economic data, some employment sizes were represented by a letter which stood for a range of values (ex. “A” meant an establishment had less than 20 employees, “B” meant an establishment may have between 20 to 99 employees, “C” means 100 to 249 employees, etc.). For these sites, the average of the range rounded up to the next integer was used for the model (ex. “A” would have 10 employees, “B” would have 60 employees, “C” would have 175 employees, etc.). This allowed for the MATLAB/GEOPHIRES model to have a numerical value to perform the calculations.
7. Another dataset included was the location of roads (Road shapefiles from the TIGER dataset). The total length of roads within each Place was used as a method to estimate the required piping length

required to service a given location (Reber, 2013) and Tester et al. (2015). Based on Reber’s conclusions, the GEOPHIRES program uses 75% road coverage to provide adequate piping density required to reach all buildings for geothermal district heating system.

8. The MATLAB script estimated the cost of a system for a lifetime of thirty years. The program uses a fixed annual charge rate (FACR), which allows the user to specify several factors, including discount rates. As reported by Shaalan (2001), this annual fixed-charge rate “represents the average or ‘levelized’ annual carrying charges including interest or return on the installed capital, depreciation or return of the capital, tax expense, and insurance expense associated with the installation of a particular generating unit” (Shaalan, 2001). A FACR of 6% was used for this Play Fairway Analysis effort. According to the U.S. Department of Commerce it calculated an effective discount rate of 3% in 2011 for Federal and Public energy projects. Therefore 1% was also added to this value, resulting in a discount rate of 4% applied to SLCOH.

9. The GEOPHIRES result output of SLCOH is a spreadsheet (.csv format). The output was grouped by state and then sorted based on the population size and the resulting SLCOH in the units of dollars per one million BTU (British Thermal Unit). \$/MMBTU. For all Places with a population of less than 4000 the SLCOH was assigned an arbitrary but high value of \$100/MMBTU. This allows us to continue to keep smaller communities in the workflow as we get ready for Phase 2. We will be able to improve our cost estimates for the entire Place list, since the GEOPHIRES and MATLAB programs allow updates for a few or many sites with the same amount of effort.

For the resulting 248 Places assessed, the best case (least expensive SLCOH) is 7 \$/MMBTU and the highest (most expensive SLCOH) is 65 \$/MMBTU. The Places were differentiated into three thresholds with the best case scenario for the SLCOH between \$7 and \$13.5, good between \$13.5 and \$16, and low or unlikely potential as \$16 to \$25 SLCOH. The distribution of the 248 Places are displayed in the Table 1 below, except for values of SLCOH over \$25 since it is considered not currently economically viable. In addition, there were 1,449 places assigned an arbitrary value for SLCOH of \$100 to separate out low populations.

Table 1: Distribution of 248 Census Places over 4,000 in population within the Appalachian Basin for NY, PA, and WV based on a three color ranking of the calculated Surface Levelized Cost of Heat (SLCOH).

State	Best Case (Green) \$5 – \$13.5/ MMBTU SLCOH	Good (Yellow) \$13.5 - \$16/ MMBTU SLCOH	Unlikely (Red) \$16 - \$25/ MMBTU SLCOH
New York	43	21	29
Pennsylvania	57	37	17
West Virginia	22	9	1

A second set of values were assigned for the five-threshold combined layer risk assessment. Here the values were \$5 to \$12 (green - best), \$12 to \$13.5 (greenish yellow), \$13.5 to \$16 (yellow), \$16 to \$20 (orange) and \$20+ (red - worst). At the level of this Phase 1 project there is not enough site knowledge, even at the

Place level, to assign increased levels of significance in the dollars amounts for the SLCOH. These were developed for the consistency of the combined risk task input files (see Catalog of Supporting Files for the [Combining Risk Factors Memo](#)).

For a comparison with current costs of energy, the FERC price of gas for New England states during the winter of 2014 was \$11.75/ MMBTU (DOE Federal Energy Regulatory Commission, 2013). This is only the price for the fuel, not all the additional infrastructure necessary for the heating/cooling of a building taken into consideration as it is within the SLCOH.

Error estimates for the Utilization risk factor were not calculated. Rather for the level of detail of Phase 1, the entire area is given a uniform uncertainty of approximately 5% based on changes in population and cost. There are inherent uncertainties for Census tract data that are similar for all of the data, such as movement between tracts or building occupancy. The Census Bureau already includes within their Place data a correction, which takes into consideration the weights for nonresponse and the sampling error (U.S. Census Bureau, 2000). The state populations of NY and PA grew 1.9% and 0.7% respectively between 2010 and 2015 and WV decreased by -0.1% during the same time period (U.S. Census Bureau, 2015). The cost of surface infrastructure and equipment is based on the cost estimates used by Reber (2013) and (Reber, Beckers, & Tester, 2014; Tester et al., 2015) that were best estimates at that time. Since 2013 the Social Security Administration has given a cost of living increase of 1.5% in 2014 and 1.7% in 2015 (Social Security Administration, 2015). Until we determine a site specific project and are able to include the below ground information, the incompleteness of this economic analysis completely overshadows the impacts of these listed errors in the pricing. Utilization risk for the SLCOH can change, but at the Phase 1 level of this project the calculations for the overall high-density heat demand of an area will not significantly change.

In fact, the Utilization demand for the heat is potentially the most known risk factor of the GPFA Appalachian Basin project. During Phase two of the project the Utilization team can work within the narrower areas of interest to differentially look at the sites under consideration. On a one-by-one basis individual site uncertainty becomes necessary for prospective development locations. Items such as Government regulations (EPA), tax incentives (state, local), green awareness/desire of industry and/or community, areas of high economic growth, building codes, local competition of infrastructure materials, cost of electricity/fossil fuels, etc., are all to be considered during the final site(s) project implementation in Phase 3 of this project.

Methodology Changes and Improvements

An improvement on the Utilization programming included an updated shell interface for the MATLAB code to allow repeated iterations of the GEOPHIRES model with a single command. This MATLAB shell module is responsible for (1) reading all required inputs from an input *.csv spreadsheet; (2) performing preliminary calculations including estimating temperature and demand profiles, reinjection temperatures, required mass flow rates, surface infrastructure equipment sizes and costs, and pumping costs; (3) executing the GEOPHIRES software package with the appropriate inputs and rerunning it if need be to ensure accurate results; (4) storing pertinent variables, including the GEOPHIRES output LCOH, and writing them to an output spreadsheet; and (5) iterating the entire workflow for each town, community or other 'Place' of interest in the study group.

Results of the SLCOH Ranking

For the Surface Levelized Cost of Heat analysis, we started with 3,355 U.S. Census Places for the three states. Of these Places, 1,697 were located within the project area. Of those Places 1,449 had populations

of less than 4,000, thus leaving 248 Places for the Utilization assessment. The lower the SLCOH of a project Place, the improved overall project economics. The SLCOH is based on a 30 year system lifetime.

The top sites for each of the three states based on the Place analysis methodology described above are listed in Table 2, Table 3 and Table 4. The results for West Virginia include the smallest populations with lowest SLCOH. This, combined with the fact that the vicinity also has several wood drying sites appearing on the Prospect List of possible industrial users, gives sites within West Virginia the best ranking for Utilization. Morgantown, with the West Virginia University interested in converting its district heating system has one of the higher rankings for the entire state. Another site of interest includes Kingwood (population 2,939 residents), site of Camp Dawson, ranked in the lower half of the WV results, yet it is still a good candidate because of the existing district heating system and interest of converting it to geothermal.

The top ten Places are county subdivision in New York and Pennsylvania, as the general populations is well above the 4000 population thresholds in the Appalachian Basin (Tables 2-4). In New York the largest cities are Buffalo, Erie County (261,000 pop) and Rochester, Monroe County (211,000 pop) within the top Places. The top counties for New York also include dairy processing sites as well as numerous colleges and universities such as Buffalo State College and University of Rochester (Table 3). Within the top locations for the state of Pennsylvania there are also many colleges, e.g., Washington & Jefferson College, Seton Hill University, Saint Vincent College, Gannon University. Pennsylvania has two of the largest populations within the Appalachian Basin project with Pittsburgh, Allegheny County (305,000 pop) and Erie, Erie County (102,000 pop). The city of Pittsburgh has multiple green initiatives such as Sustainable Pittsburgh and District 2030.

Table 2: Top ten West Virginia areas with lowest SLCOH among census areas of 4,000 and above.

County	City	Population	SLCOH (\$/MMBTU)
Lewis County	Weston city	4110	7.0
Randolph County	Elkins city	7094	11.0
Upshur County	Buckhannon city	5639	11.1
Ohio County	Wheeling city	28,486	11.2
Wood County	Parkersburg city	31,492	11.2
Monongalia County	Morgantown city	29,660	11.3
Wetzel County	New Martinsville city	53,66	11.3
Hancock County	Weirton city	19,746	11.3
Marion County	Fairmont city	18,704	11.4
Kanawha County	Charleston city	51,400	11.4

Table 3: Top ten New York areas with lowest SLCOH among census areas of 4,000 and above.

County	City	Population	SLCOH (\$/MMBTU)
Cayuga County	Auburn city	27,687	10.2
Erie County	Buffalo city	261,310	11.0
Monroe County	Rochester city	210,565	11.2
Erie County	Kenmore village	15,423	11.2
Erie County	Lancaster village	10,352	11.3
Erie County	Eggertsville CDP	15,019	11.3
Erie County	Tonawanda CDP	58,144	11.6
Oswego County	Oswego city	18,142	11.7
Cattaraugus County	Olean city	14,452	11.7
Erie County	Cheektowaga CDP	75,178	11.8

Table 4: Top ten Pennsylvania areas with lowest SLCOH among census areas of 4,000 and above.

County	City	Population	SLCOH (\$/MMBTU)
Indiana County	Indiana borough	13,975	9.9
Warren County	Warren city	9710	11.0
Washington County	Washington city	9710	11.0
Allegheny County	Dormont borough	8593	11.2
Westmoreland County	Greensburg city	14,892	11.4
Westmoreland County	Latrobe city	8338	11.5
Erie County	Erie city	101,786	11.6
Blair County	Altoona city	46,320	11.7
Allegheny County	West View borough	6771	11.7
Allegheny County	Brentwood borough	9643	11.7

Implications of SLCOH Results

All three states have numerous census Places with sufficient population within reach of geothermal district heating resources. New York has some of the highest average prices for electricity in the country, particularly in the residential sector, as reported by the Energy Industry Association (EIA) (Table 5). New York has the highest residential and commercial rates of the three states and West Virginia has the least expensive electricity, and is nationally one of the lowest in the nation. WV uses the coal mined in the state that is now going to be impacted by the new 2015 EPA Clean Power Plan (EPA, 2015). The West Virginia plan goal is to reduce their carbon dioxide emissions 29% by 2030 from their 2012 level (EPA – WV, 2015). Although, according to the coal industry, West Virginia is leading the Southern States Energy Board in rejecting the EPA Clean Power Plan and support the legal challenge by state governments against the plan (Coal Forum, 9.28.15). The Pennsylvania plans to reduce their CO₂ by 23% and New York by 10% (EPA, 2015).

Table 5: Comparison of Retail Electricity Prices for New York, Pennsylvania, and West Virginia and a Comparison between these /kW-hr and the % of the National Average Rate.

	2014 Average Retail Price of Electricity (cents per kilowatt-hour)				State Electricity Price as % of National Price		
	US	NY	PA	WV	NY	PA	WV
All Sectors	10.45	16.25	10.29	7.65	156	98	73
Residential	12.50	20.04	13.34	9.33	160	107	75
Commercial	10.75	16.11	9.72	7.99	150	90	74
Industrial	7.01	6.50	7.42	5.87	93	106	84
Transportation	10.27	13.70	7.70	9.11	133	75	89
Regional Cost Higher than National Average-More Favorable to Alternatives							
Regional Lower than National Average-Less Favorable to Alternatives Based on Cost							
Source: http://www.eia.gov/electricity/data/							
Note: West Virginia, while below the national average, sources nearly all of its electricity from coal.							

Limitations of LCOH Approach – A Case for ‘Manual Prospecting’

The purpose of the SLCOH analysis was to identify areas where educational and/or outreach efforts would be most beneficial, due to the potential for utilization of geothermal district heating. However, relying on a single bulk data analysis to gauge demand for geothermal district heating within the study area would be inadequate. Indeed, an area may be completely missing from the ‘top five’ list and **still be a viable candidate for a low temperature geothermal project**. There are numerous situations where population distribution is not the only, or even the primary, predictor of demand for geothermal district heating. For instance, with less than 3,000 residents, the town of Kingwood in Prescott County, West Virginia is unlikely to justify a geothermal district heating system as a community – but just outside Kingwood is Camp Dawson, a state owned, federally funded Army Training Site. Camp Dawson is home to various West Virginia National Guard and Reserve units, as well as a Youth Challenge Program (WV-ANG, 2015). Spread over 4177 acres, Camp Dawson hosts active and reserve military training exercises, operates a conference center with auditorium and classroom facilities, provides a variety of lodging (hotel rooms and suites, multi person barracks, cottages, etc.) and dining options for large groups, and more. While Camp Dawson clearly has economies of scale to economically utilize a geothermal district heating system, their energy selection criteria are unique from many municipalities: they value any reduction in dependence on the local utility grid because of the national security benefit and they operate an environmental office charged in part with finding opportunities to preserve the environment. While not a federally owned facility, the federal funding certainly encourages implementation of Executive Order (EO) 13693, Planning for Federal Sustainability in the Next Decade (U.S. Executive Order, 2015). Further, a number of projects have previously studied the geology, hydrology, and ecology of Camp Dawson (Weston Solutions, 2014), which will may expedite moving forward to the next stages of project preparation.

To address the likelihood of commercial businesses, industries, government agencies, and universities likely to be interested yet outside of the 248 Places assessed for their SLCOH, the team also identified over 165 prospective candidate locations, like Camp Dawson, which are included as part of the [Utilization Analysis Memo](#) items. The list of >165 include industrial applications for heat (wood drying, dairy processing), large commercial and/retail facilities, university campuses, resorts, etc. Additionally, federally owned or operated facilities and Native American Tribal lands were compiled.

Steps for Inclusion of Site Specific Industrial Sites

Low temperature direct use geothermal energy has been used for numerous industries, including aquaculture, green houses, and food processing such as dehydration and dairy processing (Lienau et al., 1994). For the Appalachian Basin region and the anticipated temperatures at depths less than 3 km depth, potential users of the geothermal heat occur in the following industry categories: paper mills, wood drying kilns, dairy processing (includes yogurt and milk pasteurization products), college and university campuses, and select military locations. Typical temperature ranges for these applications are listed in Table 6.

Table 6: Site-Specific industries of interest and required temperature ranges.

Industry	Temperature Range
Dairy	Butter/Yogurt production 80 – 90 °C Traditional pasteurization 72 – 75 °C
Wood Drying	43 – 82 °C
Paper/Pulp Mills	66 - 150 °C
University/College Campus	100 - 150 °C
Military Bases/Stations	100 - 150 °C

Each industrial site was located using a Google Map search for each category, except for the locations of the dairy processing sites found on the Dairy Plants USA website. All of these potential industrial users have a component of their process(es), which could benefit from incorporating a geothermal element into their system, either by preheating or reducing electrically heated steps.

Permits

As part of the Phase 1 research, we looked into the Permitting process in order to understand the amount of time and expenses necessary for Phase 2, with the expectation that we will be drilling at least two boreholes for a district heating system in one of the three states. Geothermal energy extraction is not established in the study area, except for geothermal heat pumps, creating limited levels of legislative clarity concerning the deeper geothermal resource. For example, in Pennsylvania and West Virginia it has not been designated if geothermal energy is a mineral right or a surface right. In New York, it is not legislatively designated as a mineral, but it is at least listed as a type of drilling under the oil and gas permitting section. During Phase 2 we will work through the permitting process of the deep geothermal wells with the appropriate agencies to educate them and then assist them in expanding their forms and the permitting process.

The permitting process includes Federal, State and Local laws to follow and / or permits to file. At the Federal level, all projects must comply with the National Environmental Policy Act (NEPA). If applicable, the Clean Air Act of 1970, Clean Water Act of 1987, Endangered Species Act and National Historic Preservation Act must also be followed.

Granting of permits to drill wells is a state function, except on federal land in which case it is a federal function carried out by the Bureau of Land Management. In New York, geothermal wells >500 feet are permitted in the same manner as oil and gas wells. There are no clear guidelines for geothermal wells in Pennsylvania and West Virginia. It is expected that permitting of deep (>1 km) geothermal wells in all three states will follow the permitting process for oil and gas wells; verification of any additional permitting will occur early in Phase 2. The three state oil and gas permitting agencies include: the New York Department of Environmental Conservation Division of Mineral Resources, the Pennsylvania Department of Environmental Protection Office of Oil and Gas Management and the West Virginia Department of Environmental Quality Office of Oil and Gas.

State drilling permits involve many forms and documents including maps, spacing units, land permission, proposed drilling program, environmental assessment, nearby water users, nearby coal leases, reclamation plans, bond, fees and workers' compensation plans.

In addition to a drilling permit, permits for water removal and reinjection may also be required. States may regulate water removal, though much of the existing information concerns drinking water. The US EPA regulates re-injection of brine. Regulations such as building codes, local zoning and local roads must also be followed. Additional permits are required for the hydro-fracture procedure of wells.

Early in Phase 2 of the project we will begin meeting with the state permitting agencies to determine which of the permits referenced above will apply to our project, determine the appropriate sequence various forms need to be submitted, the associated fees etc. We have already met with the Geological Survey or equivalent in each state and plan to continue to work closely with these agencies during the permitting process.

Submission of drilling permits will occur at the beginning of Phase 3 of the project once we have approval from the Department of Energy to proceed with the Phase 3 drilling of the project. Permitting is a process that can take many months to years to accomplish and we will need to begin this process as early as possible and with as much fore-knowledge as possible.

The Camp Dawson facility is currently undergoing environmental remediation associated with munitions testing over many years of operations. The positive aspect is that much of the NEPA work for that effort could prove very helpful.

Methodology Task 5, Combination of Risk Analysis:

Once all of the risk factors were defined, they could be combined into a general measure of favorability, referred to as a play fairway metric (PFM). The method is fairly general in that risk factors are converted to the same scale using thresholds developed by each risk factor group, and then the scaled values are combined into an aggregate measure of favorability. We expanded the analysis to provide both three- and five-color maps; the five-color scheme was an attempt to include more resolution in the analysis. More discussion of the methods of combining the risk factors is given in the memo [Combining Risk Factors](#).

Steps in the Analysis

1. Scaled the risk factors (RFs) from the original values based on thresholds specified by each risk factor group, which resulted in scaled risk factors (SRFs) that are non-dimensional. The SRF had a lower bound of 0 and an upper bound of 3 or 5, depending on the number of thresholds. Points between thresholds were generally scaled linearly, so the SRF is continuous on the interval 0-3 or 0-5. Values outside of the acceptable range, for instance temperatures that are too low for direct-use heating, were assigned a value of 0. If a value was above the highest needed for use, for instance a high productivity reservoir, then it was

given the highest value of 3 or 5, depending on the map. Reservoirs were scaled linearly in log-space because the thresholds were based on orders of magnitude.

2. Used several methods to calculate the aggregated play fairway metric (PFM). The methods of combining the risk factors included the following: sum, product, and minimum. Combined risk maps based on these PFMs were produced for combinations of all four risk factors and two special cases of three risk factors only ('geologic risk factors', including Thermal, Reservoir and Seismicity factors, and 'EGS risk factors', including Thermal, Seismicity and Utilization factors).

3. Employed uncertainty values developed by the geologic risk factor groups (does not include utilization). The range of mean and uncertainty values for each risk factor were used to develop a table of the uncertainty in the SRF based on Monte Carlo simulation. The uncertainty in each SRF map was estimated based on interpolating the Monte Carlo results. Completing separate Monte Carlo simulations for each raster cell was computationally impractical and this method was reasonable for converting the uncertainty in the risk factor (RF) to the uncertainty in the scaled risk factor (SRF). The uncertainty in the PFM was then estimated using a first-order approximation of PFM as a function of the individual SRFs. See equations below. More details are provided in the memo [Combining Risk Factors](#).

4. Illustrative project locations were selected for more in-depth analysis and graphical representation. The first step was to extract the values for a single cell associated with the project location. The values of cells were extracted and the distance to the nearest project location was calculated. The maximum value of the summed value of the four risk factors within 10 km was selected as the values for the project locations. The analysis consisted of estimating the distribution of the PFM for the location based on 10,000 Monte Carlo replicates. This allows project locations to be compared, with their estimated uncertainty, which is informative for decision makers. The main report contains a parallel axis plot (Figure 24), which shows the SRFs for each of nine illustrative locations. This represents most of the information for a project location and can show tradeoffs from one location to another. Figure 25 in the main report shows the box plot of the same nine illustrative locations for the three geologic risk factors.

Summary of the Strengths and Limitations of the Process

Any attempt to combine different dimensions of a project, without a complete physical and economic analysis for a site, will involve critical approximations. Strengths of the simple 4 risk factor analysis are that it provides several maps that could represent different ways a decision maker might consider combining the different factors. The values of each factor can also be represented spatially, which gives insight into where different factors are favorable. This allows identification of potentially favorable locations. Once a few especially attractive locations are identified, the decision maker can be presented additional site-specific information including the uncertainty distribution of the four risk factors and if the combined metric.

This analysis is limited in several ways. First, the combined PFMs are only relative representations of favorability because there is no unified economic model and the thresholds are not uniformly specified across risk factors. If there was information on the economic costs of seismic insurance, for instance, then this could be incorporated into a single model, but this is not feasible in a preliminary screening analysis. We have implied equal weighting, but some risk factors might have much more impact on the economics of a project.

Thresholds were not uniformly assigned from one risk factor to another. For instance, a value of 2 in thermal does not imply the same level of favorability as a value of 2 for seismic. The thresholds used in scaling are relative rankings and are reasonable measure of general favorability, but they will cause the result to only represent relative favorability in the combined PFM.

The uncertainty of the values is often not verifiable and were assigned based on professional judgment of the people who developed the risk factor. Therefore, our estimates of the uncertainty of the combined metric is also uncertain and represents the assessment of the developers as to the relative precision of different factors. The intent is to improve the characterization of uncertainty in phase 2.

Mathematics Used, Including Formulas and Calculation Methods

All of the calculations are for values of the scaled risk factors (SRFs) where 0 is the least favorable.

The methods of calculating the aggregated play fairway metric (PFM) were: Sum, Product, and Minimum. The equations are given below, where SRF is the scaled risk factor (scaled [0,3] or [0,5] depending on the resolution of the thresholds) and n is the number of risk factors. Generally, n=4 for the maps but in a few cases n = 3 when one risk factor is omitted.

$$PFM_{sum} = \sum_{i=1}^n SRF_i \quad \text{Equation 3}$$

$$PFM_{product} = \prod_{i=1}^n SRF_i \quad \text{Equation 4}$$

$$PFM_{minimum} = \min\{SRF_1, SRF_2, \dots, SRF_n\} \quad \text{Equation 5}$$

The uncertainty for the combined map can be approximated using a first-order Taylor series expansion along with the standard deviation assigned to each factor SRF_i . This is only applicable for the sum and product because these are “smooth” functions. The Taylor series approximation is not a good representation of the minimum and other closed-form solutions, for the variance of the minimum of four values from different distributions are not readily available. Because the distribution of each SRF is different, no general analytic results are provided for the uncertainty of the minimum. The equation used in the approximation is given below, where m is the mean value of the SRF and the variance of each SRF_i is approximated by interpolating a table derived from Monte Carlo.

$$\text{Var}(PFM) = \sum_{i=1}^n \left[\frac{\partial PFM(m)}{\partial SRF_i} \right]^2 \text{Var}(SRF_i) \quad \text{Equation 6}$$

Note: The distributions of the PFM at the individual project locations (step 4 above) were derived from Monte Carlo simulation for that specific site.

Potential Sources of Error

There are several sources of error. First, the calculations of a PFM will not exactly represent the favorability of the location. Second, the calculated values are only as good as the input, so errors from the input risk factors will probably propagate through the SRF calculated and into the PRM calculations. The uncertainty of the product map is subject to the first-order Taylor Series approximation, which is only accurate when the PFM is summed.

Software Used, Including Version and Hardware Requirements

- R: A Language and Environment for Statistical Computing, version 2.15.1 (2012-06-22, “Roasted Marshmallows”)
Packages: sp, raster, rgdal, rasterVis, maps, maptools, xlsx, rgeos, RcolorBrewer, pracma
- ArcGIS, version 10.2.2

Robustness of Different PFMs

The memo [Combining Risk Factors](#) gives some results for the robustness of the different PFMs. We would like the results to be generally the same regardless of which PFM function was selected. The three PFMs (sum, product, minimum) were calculated and extracted for each of the census “Places” that had a population greater than 4,000, indicating a reasonable utilization target. Generally, the relative rankings for the metrics are similar. The mean-product and product-minimum relationships seem especially likely to give similar relative rankings. The relative rankings could be the same but the colors might look different because of the thresholds.

METHODOLOGY REFERENCES

- AAPG. (1985). Northern Appalachian Region correlation chart. D.G. Patchen, K.L. Avary, and R.B. Erwin, regional coordinators.
- AAPG. (1985). Southern Appalachian Region correlation chart. D.G. Patchen, K.L. Avary, and R.B. Erwin, regional coordinators.
- Aguirre, G. A. (2014). *Geothermal Resource Assessment: A Case Study of Spatial Variability and Uncertainty Analysis for the State of New York and Pennsylvania*. Master's Thesis, Cornell University. Retrieved from <http://hdl.handle.net/1813/38982>
- Aguirre, G. A., Stedinger, J. R., & Tester, J. W. (2013). Geothermal Resource Assessment: A Case Study of Spatial Variability and Uncertainty Analysis for the State of New York and Pennsylvania. *Proceedings, Thirty-Eighth Workshop on Geothermal Reservoir Engineering*. Stanford: Stanford University. Retrieved from <http://www.geothermal-energy.org/pdf/IGAstandard/SGW/2013/Aguirre.pdf>
- Augustine, C. (2014). Analysis of Sedimentary Geothermal Systems Using an Analytical Reservoir Model. *Geothermal Resources Council Transactions*. Portland: Geothermal Resources Council.
- Beckers, K. F. (2015). *GEOPIHRES Software Tool*. Retrieved from GEOthermal Energy for the Production of Heat and Electricity Economically Simulated: <http://koenraadbeckers.net/geophires/index.php>
- Beckers, K. F., Lukawski, M. Z., Anderson, B. J., Moore, M. C., & Tester, J. W. (2014). Levelized costs of electricity and direct-use heat from Enhanced Geothermal Systems. *Journal of Renewable and Sustainable Energy, Vol. 6, No. 1*, 013141.
- Beckers, K. F., Lukawski, M. Z., Reber, T. J., Anderson, B. J., Moore, M. C., & Tester, J. W. (2013). Introducing GEOPIHRES V1.0: Software Package For Estimating Levelized Cost of Electricity and/or Heat from Enhanced Geothermal Systems. *Proceedings, Thirty-Eighth Workshop on Geothermal Reservoir Engineering*. Stanford: Stanford University. Retrieved from <http://www.geothermal-energy.org/pdf/IGAstandard/SGW/2013/Beckers.pdf>
- Bedre, M., & Anderson, B. (2012). Sensitivity analysis of low-temperature geothermal reservoirs: effect of reservoir parameters on the direct use of geothermal energy. *Geothermal Resources Council Transactions* (pp. 1255-1262). Geothermal Resources Council.
- Blackwell, D. (n.d.).
- Blackwell, D. D., & Richards, M. (Eds.). (2004). 2004 Geothermal Map of North America, Scale 1:6,500,000. American Association of Petroleum Geologists.
- Blackwell, D. D., & Richards, M. (2004). Geothermal Map of North America; Explanation of Resources and Applications. *Geothermal Resources Council Transactions*, 28 (pp. 317-320). Geothermal Resources Council.
- Blackwell, D. D., Richards, M., Batir, J., Frone, Z., & Park, J. (2010). New Geothermal Resource Map of the Northeastern US and Technique for Mapping Temperature-at-depth. *Geothermal Resources Council Transactions, Vol. 34* (pp. 313-318). Geothermal Resources Council.

- Blackwell, D. D., Richards, M., Frone, Z., Batir, J., Ruzo, A., Dingwall, R., & Williams, M. (2011). Temperature-At-Depth Maps for the Conterminous U.S. and Geothermal Resource Estimates. *Geothermal Resources Council Transactions, Vol. 35* (pp. 1545-1550). Geothermal Resources Council.
- Blackwell, D., Richards, M., Frone, Z., Batir, J., Ruzo, A., Dingwall, R., & Williams, M. (2011). Temperature-At-Depth Maps for the Conterminous U.S. and Geothermal Resource Estimates. *Geothermal Resources Council Transactions, Vol. 35* (pp. 1545-1550). Geothermal Resources Council.
- Boschetti, F., Hornby, P., & Horowitz, F. (2001). Wavelet Based Inversion of Gravity Data. *Exploration Geophysics, 32*(1), 48-55. doi:10.1071/EG01048
- Buescher, E. (. (2015). Green District Heating - Actual Developments of Deep Geothermal Energy in Germany. *Proceedings World Geothermal Conference 2015*. Melbourne, Australia: International Geothermal Association. Retrieved from <http://www.geothermal-energy.org/pdf/IGAstandard/WGC/2015/35000.pdf>
- Byerlee, J. (1978). Friction of Rocks. *Pure and Applied Geophysics, 116*((4-5)), 615-626. doi:10.1007/bf00876528
- Camp Dawson West Virginia Army National Guard. (2015). *About Camp Dawson*. Retrieved from Camp Dawson West Virginia Army National Guard: <http://www.wv.ngb.army.mil/CampDawson/Form1.aspx?MP=MTc1&P=MTc1#Dawson>
- Carter, L., Kelley, S., Blackwell, D., & Naeser, N. (1998). Heat flow and thermal history of the Anadarko basin, Oklahoma. *American Association of Petroleum Geologists Bulletin, 82*, pp. 291-316.
- Cho, J., Augustine, C., & Zerpa, L. (2015). Validation of a Numerical Reservoir Model of Sedimentary Geothermal Systems Using Analytical Models. *Stanford Geothermal Workshop Proceedings*. Stanford University.
- DOE Federal Energy Regulatory Commission. (2013, October 17). *Winter 2013-14 Energy Market Assessment Report to the Commission, Item No. A-5*. Retrieved from <http://www.ferc.gov/CalendarFiles/20131017101835-2013-14-WinterReport.pdf>
- Engelder, T., Lash, G., & Uzcátegui, R. (2009). Joint sets that enhance production from Middle and Upper Devonian gas shales of the Appalachian Basin. *AAPG Bulletin, 93*(7), 857-889.
- Förster, A., & Memam, D. F. (1995). A Bottom-Hole Temperature Analysis in the American Midcontinent (Kansas): Implications to the Applicability of BHTs in Geothermal Studies. (pp. 777-782). Potsdam: International Geothermal Association.
- Frone, Z. (2015). *Heat Flow, Thermal Modeling and Whole Rock Geochemistry of Newberry Volcano, Oregon and Heat Flow Modeling of the Appalachian Basin, West Virginia*. Southern Methodist University. ProQuest Dissertations Publishing.
- Frone, Z., & Blackwell, D. (2010). Geothermal Map of the Northeastern United States and the West Virginia Thermal Anomaly. *Geothermal Resources Council Transactions, V. 34* (pp. 339-343). Geothermal Resources Council.

- Gallardo, J., & Blackwell, D. (1999). Thermal structure of the Anadarko Basin, Oklahoma. *American Association of Petroleum Geologists Bulletin*, 83, pp. 331-361.
- Gerard, A., Genter, A., Kohl, T., Lutz, P., Rose, P., & Rummel, F. (2006). The Deep EGS (Enhanced Geothermal System) Project at Soultz-sous-Forets (Alsace, France). *Geothermics, Volume 35*, 473-483.
- GoldCorp Inc. (2001, March 12). US\$575,000 Goldcorp Challenge Awards world's first 6 million ounce internet gold rush yields high grade results! Toronto. Retrieved from <http://www.infomine.com/index/pr/Pa065434.PDF>
- Gringarten, A. (1978). Reservoir lifetime and heat recovery factor in geothermal aquifers used for urban heating. *Pure and Applied Geophysics*, 117 (1-2), 297-308.
- Harrison III, W., Grammer, G., & Barnes, D. (2009). Reservoir characteristics of the Bass Islands dolomite in Otsego County, Michigan: Results for a saline reservoir CO2 sequestration demonstration. *Environmental Geosciences, Vol. 16, No. 3*, 139-151.
- Harrison, W., Luza, K., Prater, M., & Chueng, P. (1983). Geothermal Resource Assessment of Oklahoma. *Special Publication 83-1, Oklahoma Geological Survey*.
- He, X. (2015). *Feasibility and Supply Analysis of U.S. Geothermal District Heating and Cooling Systems*. West Virginia University, Benjamin M. Statler College of Engineering and Mineral Resources. Morgantown: Proquest LLC, UMI Dissertation Publishing. Retrieved from <http://search.proquest.com/docview/1682034532>. Abstract Available at <http://gradworks.umi.com/37/01/3701975.html>
- Hildenbrand, T. G., Briesacher, A., Flanagan, G., Hinze, W. J., Hittelman, A. M., Keller, G. R., . . . Webring, M. (2002). *Rationale and Operational Plan to Upgrade the U.S. Gravity Database*. Retrieved from Gravity Database of the US: <http://research.utep.edu/default.aspx?tabid=37229>
- Hornby, P., Boschetti, F., & Horowitz, F. (1999, April). Analysis of potential field data in the wavelet domain. *Geophysical Journal International*, 137(1), 175-196. doi:10.1046/j.1365-246x.1999.00788.x
- Hornby, P., Horowitz, F., & Boschetti, F. (2002). A Physical Interpretation of the Poisson Wavelet Transform of Potential Fields. *Proceedings, EGS XXV!! General Assembly*. Munich: European Geophysical Society. Retrieved from <http://www.cosis.net/abstracts/EGS02/05568/EGS02-A-05568.pdf>
- Jaeger, J. C. (1965). Application of the theory of heat conduction to geothermal measurements. In W. H. Lee (Ed.), *Terrestrial Heat Flow*. Washington, D.C.: American Geophysical Union. doi:10.1029/GM008p0007
- Lachenbruch, A. (1968). Preliminary geothermal model of the Sierra Nevada. *Journal of Geophysical Research*, 73(2), 6977-6989.
- Lewis, J., McDowell, R., Avary, K., & Carter, K. (2009). Characterization of the Helderberg Group as a geologic seal for CO2 sequestration. *Environmental Geosciences, Vol. 16, No. 4*, 201-210.
- Lienau, P., Lund, J., Rafferty, K., & Culver, G. (1994). *Reference Book on Geothermal Direct Use* (Vol. August). Klamath Falls, Oregon: GGeo-Heat Center, Oregon Institute of Technology. Retrieved

- from <http://www.oit.edu/docs/default-source/geoheat-center-documents/publications/direct-use/tp82.pdf?sfvrsn=2>
- Lindal, B. (1973). Industrial and other applications of geothermal energy (except power production and district heating). *Geothermal Energy; Review of Research and Development*.
- Lugert, C., Smith, L., Nyahay, R., Bauer, S., & Ehgartner, B. (2006). *Systematic Technical Innovations Initiative Brine Disposal in the Northeast*. Albany, NY: New York State Energy Research and Development Authority.
- Malinconico, L., & Moore, M. (2013). *Provisional Bouguer Gravity Map of Pennsylvania*. Retrieved from AASG Geothermal Data Repository: <http://repository.stategeothermaldata.org/repository/resource/a748ce233a25e3e0dd00c9865d0af3e5/>
- Mardia, K. (1972). *Statistics of Directional Data*. Academic Press. Retrieved from <http://www.worldcat.org/isbn/9780124711501>
- Midwest Regional Carbon Sequestration Partnership. (2009). *Phase II Report*. Midwest Regional Carbon Sequestration Partnership. Retrieved from http://www.mrcsp.org/userdata/phase_ii_reports/phase_ii_final_report_MRCSP.pdf
- Nelson, P. H. (2009). Pore-throat sizes in sandstones, tight sandstones, and shales. *AAPG Bulletin*, v. 93, no. 3, 329-340.
- Obama, B.H. (2015). *Executive Order 13693 - Planning for Federal Sustainability in the Next Generation*. Washington, D.C.: U.S. Government Publishing Office. Retrieved 2015, from <http://www.gpo.gov/fdsys/pkg/FR-2015-03-25/pdf/2015-07016.pdf>
- Pebesma, E. J., & Wesseling, C. G. (1998). Gstat, a program for geostatistical modelling, prediction and simulation. *Computers & Geosciences*, 24 (1), 17-31.
- Ravat, D., Finn, C., Hill, P., Kucks, R., Phillips, J., Blakely, R., . . . Elawadi, E. (2009). *A Preliminary, Full Spectrum, Magnetic Anomaly Grid of the United States with Improved Long Wavelengths for Studying Continental Dynamics: A Website for Distribution of Data*. United States Geological Survey. Retrieved from <http://pubs.usgs.gov/of/2009/1258>
- Reber, T. J. (2013). *Evaluating Opportunities For Enhanced Geothermal System-Based District Heating In New York And Pennsylvania*. Cornell University. Ithaca, NY: Cornell University. Retrieved from <http://hdl.handle.net/1813/34090> (restricted until 2018)
- Reber, T. J., Beckers, K. F., & Tester, J. W. (2014). The transformative potential of geothermal heating in the U.S. Energy market: a regional study of New York and Pennsylvania. *Energy Policy*, Vol. 70, 30-44.
- Roen, J., & Walker, B. (1996). The atlas of major Appalachian gas plays. *Publication V-25*.
- Roy, R. F., Blackwell, D. D., & Birch, F. (1968). Heat generation of plutonic rocks and continental heat flow provinces. *Earth and Planetary Science Letters*, 5, 1 – 12.
- Roy, R. F., Blackwell, D. D., & Decker, E. R. (1972). Continental heat flow. In E. E.C. Robertson (Ed.), *The Nature of the Solid Earth* (pp. 506-44). New York: McGraw Hill.

- Sanyal, S., & Butler, S. (2009). Geothermal Power From Wells in Non-Convective Sedimentary Formations - An Engineering Economic Analysis. *Geothermal Resources Council Transactions, Vol. 33* (pp. 865-870). Geothermal Resources Council.
- Shaalán, H. E. (2001). Generation of Electric Power. In *Handbook of Electric Power Calculations* (pp. 8.1-8.38). Retrieved from http://castlelab.princeton.edu/EnergyResources/GenerElectPower__Shalaan.pdf
- Shope, E. N. (2012). *A Detailed Approach To Low-Grade Geothermal Resources In The Appalachian Basin Of New York And Pennsylvania: Heterogeneities Within The Geologic Model And Their Effect On Geothermal Resource Assessment*. Master's Thesis, Cornell University. Retrieved from <http://hdl.handle.net/1813/31206>
- Shope, E. N., Reber, T., Stutz, G., Aguirre, G., Jordan, T., & Tester, J. (2012). Geothermal Resources Assessment: A Detailed Approach to Low-Grade Resources in the States of New York and Pennsylvania. *PROCEEDINGS, Thirty-Seventh Workshop on Geothermal Reservoir Engineering*. 37. Stanford: Stanford University. Retrieved from <https://pangea.stanford.edu/ERE/pdf/IGAstandard/SGW/2012/Shope.pdf>
- Smith, L., Nyahay, R., & Slater, B. (2010). *Integrated Reservoir Characterization of the Subsurface Cambrian and Lower Ordovician Potsdam, Galway and Theresa Formations in New York*. New York State Energy Research and Development Authority (NYSERDA).
- Social Security Administration. (2015). *Cost-Of-Living Adjustment, Prior Cost-of-Living Adjustments*. Retrieved from Official Social Security Website: <http://www.ssa.gov/news/cola/facts>
- Spicer, H. C. (1964). A compilation of deep earth temperature data, U. S. A. 1910-1945. *Open-File Report 64-167, U.S Geological. Survey*.
- Stutz, G. R. (2012). *Development, Analysis, and Application of a Well by Well Method for Estimating Surface Heat Flow for Regional Geothermal Resource Assessment*. Cornell Thesis, Cornell University. Retrieved from <http://hdl.handle.net/1813/31037>
- Stutz, G. R., Williams, M., Frone, Z., Reber, T., Blackwell, D., Jordan, T., & Tester, J. (2012). A Well by Well Method for Estimating Surface Heat Flow for Regional Geothermal Resource Assessment. *Stanford Geothermal Workshop Proceedings*. Stanford University.
- Stutz, G., Williams, M., Frone, Z., Reber, T., Blackwell, D., Jordan, T., & Tester, J. (2012). A Well by Well Method for Estimating Surface Heat Flow for Regional Geothermal Resource Assessment. *Stanford Geothermal Workshop Proceedings*. Stanford University.
- Tester, J., Joyce, W., Brown, L., Bland, B., Clark, A., Jordan, T., . . . Anderson, B. (2010). Co-generation Opportunities for Lower Grade Geothermal Resources in the Northeast - A Case Study of the Cornell Site in Ithaca, NY. *GRC Transactions*. 34, pp. 475-483. Geothermal Resources Council. Retrieved from <http://pubs.geothermal-library.org/lib/grc/1028690.pdf>
- Tester, J., Reber, T., Beckers, K., Lukawski, M., Camp, E., Aguirre, G. A., . . . Horowitz, F. (2015). Integrating Geothermal Energy Use into Re-building American Infrastructure. *Proceedings World Geothermal Congress*. Melbourne, Australia: International Geothermal Association. Retrieved from <http://www.geothermal-energy.org/pdf/IGAstandard/WGC/2015/38000.pdf>

- The Coal Forum. (2015, 10 01). *WV Leads SSEB in Rejecting 'Clean Power Plan'*. Retrieved from [wwwcoalforum.org](http://www.wvcoalforum.org): <http://www.wvcoalforum.org/201510015019/recent-press/wv-leads-sseb-in-rejecting-clean-power-plan.html>
- U.S. Census Bureau. (2000, Created 2003, Last Revised 2004, Accessed 2015). *U.S. Census Bureau*. Retrieved from Survey of Program Dynamics, Sampling Errors: <http://www.census.gov/spd/sampling.html>
- U.S. Census Bureau. (2015). *U.S. Census Bureau*. Retrieved from State Quick Facts: <http://quickfacts.census.gov/qfd/states/>
- U.S. Energy Information Administration . (2015, October 1). *Frequently Asked Questions, Estimated U.S. residential electricity consumption by end use, 2014*. Retrieved from U.S. Energy Information Administration: <http://www.eia.gov/tools/faqs/faq.cfm?id=96&t=3>
- U.S. Environmental Protection Agency (EPA). (2015, 8 3). *U.S. Environmental Protection Agency (EPA)*. Retrieved from Clean Power Plan: State at a Glance, West Virginia: <http://www3.epa.gov/airquality/cpptoolbox/west-virginia.pdf>
- U.S. Environmental Protection Agency (EPA). (2015, 10 01). *U.S. Environmental Protection Agency (EPA)*. Retrieved from Clean Power Plan for Existing Power Plants: <http://www2.epa.gov/cleanpowerplan/clean-power-plan-existing-power-plants>
- U.S. Geoscience Information Network. (2015, August 27). *USGIN Content Model Schemas Geologic Reservoir 1.0*. Retrieved from <http://schemas.usgin.org/models/#geologicreservoir>
- Walcott, C. (1896). *Cambrian Rock of Pennsylvania*. United States Geological Survey (USGS). Retrieved from <http://pubs.usgs.gov/bul/0134/report.pdf>
- West Virginia Geological & Economic Survey. (2006). *Trenton Black River Project Appalachian Basin*. Retrieved from Trenton-Black River Project Website: <http://www.wvgs.wvnet.edu/www/tbr/>
- Weston Solutions, Inc. (2014, June). *Engineering Evaluation/Cost Analysis Known Distance Range Munitions Response Site Berm Area*. Contract No. : W912DR-09-D-006, Delivery Order No.: 0008, West Chester, PA. Retrieved 9 2015, from West Virginia Army National Guard: http://www.wv.ngb.army.mil/CampDawson/Documents/kd_range_final.pdf
- Wheaton, C. (2015). *Statistical Correction of Temperature Data for New York and Pennsylvania Wells*. M.S. Thesis, Cornell University, Ithaca. Retrieved from <http://hdl.handle.net/1813/40609>
- Zoback, M. D., Barton, C. A., Brudy, M., Castillo, D. A., Finkbeiner, T., Grollimund, B. R., . . . Wiprut, D. J. (2003). Determination of stress orientation and magnitude in deep wells. *International Journal of Rock Mechanics and Mining Sciences*, Vol. 40 No. 7, 1049-1076.